The Journal of the Korean Society of Oceanography
Vol. 32, No. 2, pp. 75-84, June 1997

On the Length Scale and the Wall Proximity Function in the Mellor-Yamada Level 2.5 Turbulence Closure Model for Homogeneous Flows

JONG CHAN LEE AND KYUNG TAE JUNG*
Korea Ocean Research and Development Institute, Ansan P.O. Box 29, Ansan 425-600, Korea

Relation between the length scale and the wall proximity function in the Mellor-Yamada level 2.5 turbulence closure model has been investigated through various experiments using a range of wall proximity functions. The model performance has been evaluated quantitatively by comparing with laboratory data for wind-driven flow (Baines and Knapp, 1965) and for open-channel flows without and with adverse wind action (Tsuruya, 1985). Comparison shows that a symmetric wall proximity function used by Blumberg and Mellor(1987) gives rise to current profiles with better accuracy than asymmetric wall proximity functions considered. It is noted that in modelling homogeneous flows the length scale $l = 0.31|z|(1+z/h)$ can be used with tolerable accuracy.

INTRODUCTION

An unique feature of POM (Princeton Ocean Model) is that a turbulence closure submodel on the basis of the Mellor and Yamada level 2.5 model (hereafter MY level 2.5 model) is imbedded. However, its application has been mostly confined to simulating processes in stratified situations. Only a small amount of work has been done using the turbulence model for the homogeneous, unstratified flows in shelf and coastal sea regions (for example, Xing and Davies, 1996).

Originally, the MY level 2.5 model based on the second-moment closure of turbulence assumes that all length scales be everywhere proportional to each other (they said it was their greatest weakness). The proper prescription of the length scale containing complex correlations whose behavior is little known, is one of the major unresolved issues in turbulence modelling (Kantha and Clayson, 1994). Although the MY level 2.5 model has been successfully applied to various problems in coastal and oceanic phenomena, no rigorous work on the length scale has been done in the simulation of homogeneous flows particularly under presence of wind action.

In this paper, the performance of the MY level 2.5 model with a range of wall proximity functions is investigated through various experiments. We first carry out point model experiments for wind-driven and tidal currents in a homogeneous unbounded deep ocean. Besides, the model performance has been evaluated quantitatively by comparing with laboratory data for wind-driven flow in a closed channel (Baines and Knapp, 1965) and for flow-controlled channel flows without and with adverse wind action (Tsuruya, 1985). Special attention has been paid to the relation between the length scale and wall proximity functions.

THE MY LEVEL 2.5 MODEL

We briefly describe the level 2.5 turbulence energy model developed by Mellor and Yamada (1982). Details of the model are given in Blumberg and Mellor (1987).

In the MY level 2.5 model the vertical eddy viscosity K_M is given by

$$K_M = l \cdot q \cdot S_M \tag{1}$$

where l is a length scale termed the turbulence macroscale, q is a velocity scale obtained from the turbulent kinetic energy (TKE = $q^2/2$), and S_M is a dimensionless stability function.

According to the quasi-equilibrium closure of Galperin *et al.* (1988), the modified stability function (S_M) in homogeneous flows reduces to a constant; $S_M = 0.39327$. A slight small value $S_M = 0.3920(=B_1^{-1/3})$ was used by Blumberg *et al.* (1992), and this value is used in this study.

The governing equations for TKE and the length

scale in (x-z) two-dimensional flow are given by

$$\frac{\partial q^2}{\partial t}+u\frac{\partial q^2}{\partial x}+w\frac{\partial q^2}{\partial z}=2K_M\left(\frac{\partial u}{\partial z}\right)^2-\frac{2q^3}{B_1 l}+\frac{\partial}{\partial z}\left(K_q\frac{\partial q^2}{\partial z}\right)+F_q \quad (2)$$

$$\frac{\partial q^2 l}{\partial t}+u\frac{\partial q^2 l}{\partial x}+w\frac{\partial q^2 l}{\partial z}=lE_1K_M\left(\frac{\partial u}{\partial z}\right)^2-\frac{q^3}{B_1}W+\frac{\partial}{\partial z}\left(K_q\frac{\partial q^2 l}{\partial z}\right)+F_l \quad (3)$$

where t is the time, (x, z) form a Cartesian coordinate system, u is the horizontal velocity component, w is the vertical component of velocity, K_q is the eddy diffusivity of the turbulence model variables, and W is the wall proximity function. B_1(= 16.6) and E_1(=1.8) are empirical constants specified using laboratory data (Mellor and Yamada, 1982). F_q and F_l are horizontal mixing terms the expression of which is given in Blumberg and Mellor (1987) and will not be repeated here.

The wall proximity function W takes the form:

$$W=1+E_2\left(\frac{l}{kL}\right)^2 \quad (4)$$

where E_2(=1.33) is an empirical constant, k(=0.4) is the von Karman constant, L is a measure of the distance away from a boundary, the specific description of which will be discussed later.

The boundary conditions of the turbulence model variables at the sea surface (z=0) and bottom (z=-h) are:

$$(q^2, q^2l)_{z=0}=(B_1^{-2/3}u_{*s}^2, 0) \quad (5a)$$

$$(q^2, q^2l)_{z=-h}=(B_1^{-2/3}u_{*b}^2, 0) \quad (5b)$$

where u_{*s} is the surface friction velocity (= $\sqrt{\tau_w/\rho_0}$, τ_w is wind stress), u_{*b} is the bottom friction velocity (=$\sqrt{\tau_b/\rho_0}$, τ_b is bottom stress), ρ_0 is the reference water density (assumed constant).

The constants involved in the MY level 2.5 model and the boundary conditions (5a) and (5b) are derived under the assumption that turbulent energy production and dissipation are balanced, which is the assumption of level 2 in the MY hierarchy. With the assumption of level 2, the asymptotic length scale can be determined by an algebraic equation,

Table 1. Summary of measure of distance (L) in wall proximity function

Notation	Measure of distance (L) in wall proximity function	Remarks
W1	$\|z\|$	L increases from the surface
W2	$h+z$	L increases from the bottom
W3	$\|z\|\ (1+z/h)$	L is symmetric
W4	$\dfrac{\|z\|(1+z/h)}{\sqrt{(z/h)^2+E_3/E_2(1+z/h)}}$	Asymmetry of L is enforced

$$l=k\sqrt{\frac{E_1-1}{E_2}}L=0.31L \quad (6)$$

Table 1 summarizes a range of L considered in this study. The simplest form W1 was used by Deleersnijder and Luyten (1994) in numerical experiments dealing with the stress-driven deepening of the ocean mixed layer. The second form W2 is considered in this study because the asymptotic length scale is similar to those given by Blackadar (1962), and often used by researchers in tidal flow modelling (Mellor and Yamada, 1982; Mofjeld and Lavelle, 1984; Davies and Jones, 1987). Use of W3 could be found in Blumberg and Mellor (1987) for the response of stratified ocean due to wind forcing and Xing and Davies (1996) for tidal current in Irish Sea. The last one W4 was used by Blumberg *et al.* (1992) in calculating the open-channel flow to account for the effect of free surface with new coefficient E_3(=0.25). Recently it was applied to coastal circulation by Lynch *et al.* (1996) to incorporates asymmetry of the length scale among surface and bottom walls.

NUMERICAL EXPERIMENTS AND RESULTS

Wind-driven current and tidal current in open sea

The governing equations for wind-driven and tidal currents in a homogeneous unbounded ocean are

$$\frac{\partial u}{\partial t}-fv=-\frac{1}{\rho_0}\frac{\partial p}{\partial x}+\frac{\partial}{\partial z}\left(K_M\frac{\partial u}{\partial z}\right) \quad (7)$$

$$\frac{\partial v}{\partial t}+fu=-\frac{1}{\rho_0}\frac{\partial p}{\partial y}+\frac{\partial}{\partial z}\left(K_M\frac{\partial v}{\partial z}\right) \quad (8)$$

where (x, y, z) form a right-handed Cartesian coordinate system, p is pressure, (u, v) are the

horizontal velocity components and f is the Coriolis parameter.

The surface and bottom boundary conditions for the momentum equations are

$$\rho_0 K_M \left(\frac{\partial u}{\partial z}, \frac{\partial v}{\partial z} \right)_{z=0} = (\tau_w^x, \tau_w^y) \quad (9a)$$

$$\rho_0 K_M \left(\frac{\partial u}{\partial z}, \frac{\partial v}{\partial z} \right)_{z=-h} = (\tau_b^x, \tau_b^y) = \rho_0 k_f (u_b, v_b) \quad (9b)$$

where (τ_w^x, τ_w^y) are horizontal components of wind stress, (τ_b^x, τ_b^y) are horizontal components of bottom stress, k_f is a linear bottom friction coefficient (in velocity unit) and (u_b, v_b) are near-bottom velocity components.

First, simulations of wind-driven currents were carried out with input parameters: $(\tau_w^x, \tau_w^y) = (0.1, 0.1)$ N/m^2, $(\frac{\partial p}{\partial x}, \frac{\partial p}{\partial y}) = (0, 0)$, $f = 9.3 \times 10^{-5}$ s^{-1}, $h = 100$ m and $k_f = 0.005$ (m/s). In practical calculations the vertical axis was represented by a normalized coordinate, $\sigma = z/h$ and was divided equally into 100 levels. Calculations are started with condition of no motion and the time step Δt is set to 120 s.

Fig. 1 shows profiles of u, K_M, q^2 and l/h at t=60 hours. Results obtained using W1, W2, W3 and W4 are represented by lines with circles, triangles, plus and cross symbols, respectively. It is evident that surface currents subject to steady wind forcing are sensitive to the wall proximity function. Use of different wall proximity function gives considerable difference in l and consequently K_M.

It is seen that W3 produces the strongest surface

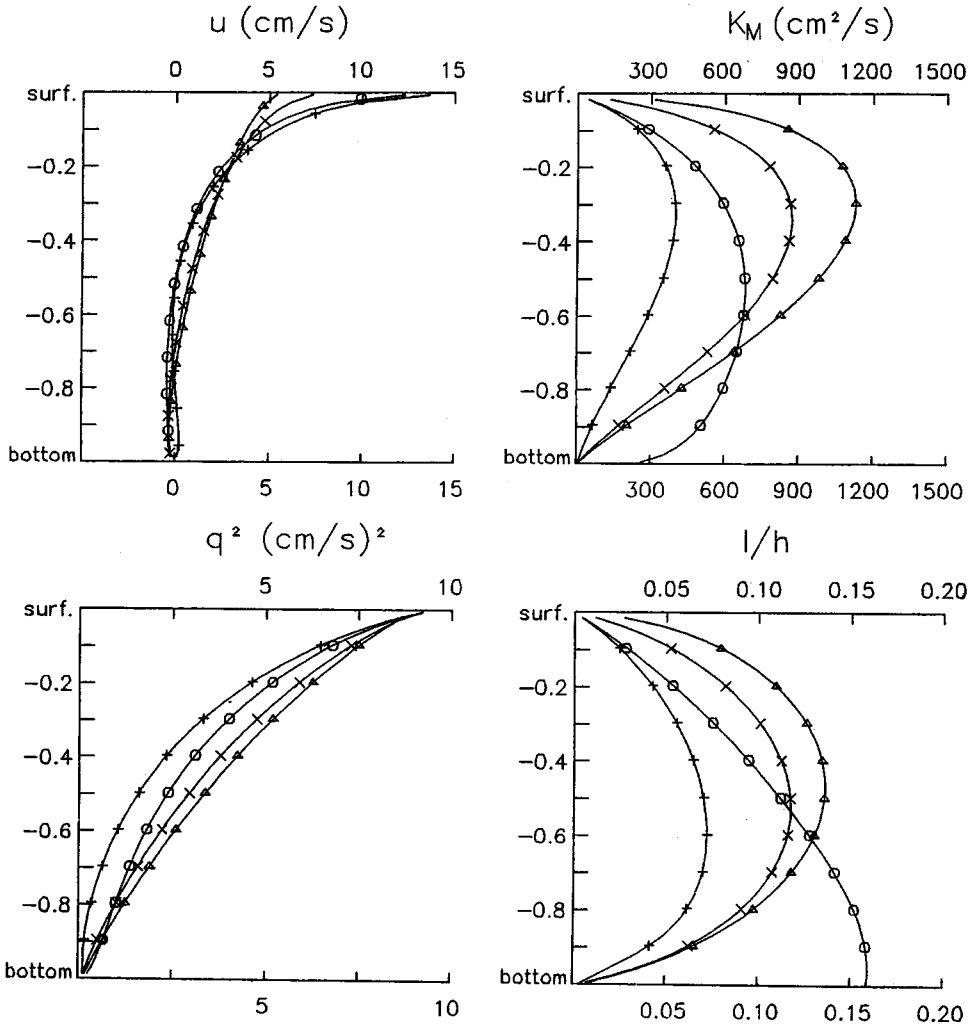

Fig. 1. Profiles of u, K_M, q^2 and l/h for wind-driven currents obtained using a point model with a range of wall proximity functions. circles: W1, triangles: W2, plus symbol: W3, cross symbol: W4.

currents with considerable vertical shear, while W2 produces the weakest surface current. Current profiles obtained using W1 are almost equivalent to those obtained using W3, and current profiles obtained using W4 are similar to those obtained using W2 except for the slight difference near the sea surface.

Changing L in the wall proximity function yields the modification of the length scale l throughout the depth, giving significant difference in its depth-mean value and profiles. The length scale obtained using W1 shows a linear profile increasing from the surface, while the length scales obtained using other wall proximity functions show parabolic profiles with a maximum at approximately mid-depth. It is noted that the length scale profile computed with W4 is almost symmetric despite the asymmetric nature of W4. Turbulent kinetic energy q^2 decreases from the surface to the bottom and are almost same in profiles and magnitudes independently of wall proximity functions.

The mean value and the near surface variation of the vertical eddy viscosity K_M are strongly affected by the form of wall proximity function. It is worth noting that K_M is mainly dependent upon l rather than q^2 (Note that l/q is an order of 10^3).

In the second experiment, oscillatory tidal currents are simulated with the pressure gradient prescribed as an external forcing, thus,

$$-\frac{1}{\rho_0}\left(\frac{\partial p}{\partial x}, \frac{\partial p}{\partial y}\right) = \omega(U_r, V_r)\cos(\omega t) \tag{10}$$

where $\omega = 1.45 \times 10^{-4}$ s^{-1} (S_2 tide) and $\omega \cdot (U_r, V_r)$ are

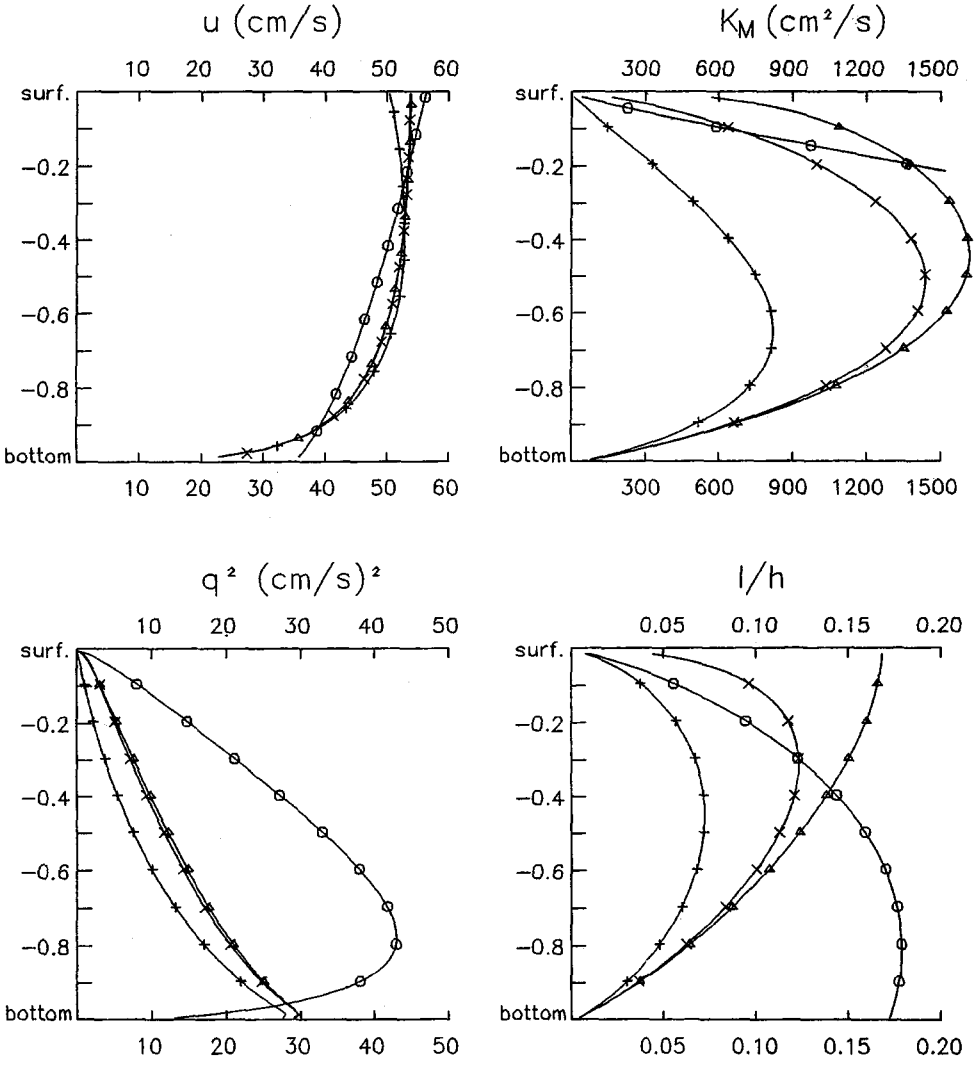

Fig. 2. Profiles of u amplitude, tide-averaged K_M, q^2 and l/h for tidal current obtained using a point model with a range of wall proximity function. Symbols are same as Fig. 1.

amplitudes of tidal forcing.

In this experiments, τ_w^x, τ_w^y, V_r and f are set to zero, U_r is set to 0.5 m/s (if the vertical diffusion term in the momentum equation could be neglected, then the amplitude of tidal current equals to U_r) and other parameters are same as those of the wind-driven current experiment.

Fig. 2 shows profiles of tidal current amplitude, tide-averaged K_M, q^2 and l/h. Profiles of near-bottom tidal current amplitude are almost similar to each other except for the case of W1. The profile of tidal current amplitude obtained using W1 shows a linear variation over the whole water column, while other profiles show a sharp gradient near the bottom but little gradient above mid-depth.

The length scale profile above the mid-depth obtained using W1 is similar to that derived by equation (6). Calculation with W2 shows a length scale profile linearly increasing from the bottom, and the ratio of l to h reaches approximately 0.16. The length scale obtained using W3 is almost identical to its asymptotic profile throughout the whole water column. It is noted that the length scale profile obtained using W4 is conspicuously asymmetric and is almost identical to its asymptotic profile even in the absence of free surface variation.

Results obtained using W2, W3 and W4 show profiles of q^2 decreasing from the bottom to the surface, while calculation with W1 shows an asymmetric profile with a maximum around σ=-0.8.

The vertical eddy viscosity K_M obtained using W1 shows a maximum value of 4400 cm^2/s at σ=-0.8. Calculation using W3 shows an asymmetric profile with a maximum value of 800 cm^2/s at σ=-0.7, while calculations using W2 and W4 show almost symmetric profiles with maximum values (1,600 cm^2/s and 1,400 cm^2/s) at mid-depth.

Wind-driven flow in closed channel

In this part, model performance has been evaluated quantitatively by comparing with laboratory data obtained by Baines and Knapp (1965).

We consider a closed channel the longitudinal direction of which equals to x coordinate. The (x-z) two-dimensional model solves continuity and x-directed momentum equation,

$$\frac{\partial \zeta}{\partial t} + \frac{\partial (H\bar{u})}{\partial x} = 0 \tag{11}$$

$$\frac{\partial u}{\partial t} + u\frac{\partial u}{\partial x} + w\frac{\partial u}{\partial z} = -g\frac{\partial \zeta}{\partial x} + \frac{\partial}{\partial z}\left(K_M \frac{\partial u}{\partial z}\right) + F_u \tag{12}$$

where

$$\bar{u} = \int_{-h}^{\zeta} u \, dz \tag{13a}$$

$$w(z) = -\frac{\partial}{\partial x}\int_{-h}^{z} u \, dz \tag{13b}$$

In the above equation ζ is the free surface elevation, g is acceleration due to gravity, H is the total water depth ($=h+\zeta$) and F_u is the horizontal diffusion term.

The channel is approximated by staggered grids. The actual calculations use a σ-coordinate $\{\sigma = (z-\zeta)/H\}$. Simulations of wind-driven flow were carried out for 400 seconds with input parameters: u_{*s} = 0.875 cm/s (τ_w^x = 0.78 N/m^2), h=32.8 cm, k_f = 0.001 (m/s), Δt = 0.25 s, Δx = 0.5 m and $\Delta\sigma$ = 0.01. The motion is again generated from a state of no motion.

Fig. 3 shows profiles of u, K_M, q^2 and l/H obtained using a range of wall proximity functions. The observed data in Baines and Knapp's experiment are represented by square symbols. It is again evident that surface current and the length scale due to steady wind forcing are significantly affected by the wall proximity function, while profiles of turbulence kinetic energy q^2 are almost similar to each other regardless of the form of wall proximity functions.

Unlike the point model experiment of wind-driven currents in an unbounded deep ocean (h=100 m), all of the length scale profiles obtained using different wall proximity functions show parabolic variations because vertical diffusion terms in q^2 and q^2l equation are not negligible in this shallow channel flow (h=32.8 cm). The ratios of l to H obtained using W2, W3 and W4 are almost identical to those of wind-driven current in an unbounded deep ocean.

The computed q^2 profiles using four wall proximity functions show little difference. It is again evident that profiles of velocity, K_M and l are considerably changed by the form of L, but profiles of q^2 are altered very slightly.

For the quantitative evaluation of model results, root mean square errors (RMSE in cm/s) are examined. The best results (RMSE=1.41) were obtained using W1, while relatively poor results (RMSE=3.33) were obtained using W2. It is noted that benefits of using W4 are marginal (RMSE=2.69) and still considerable errors can arise in reproducing velocity

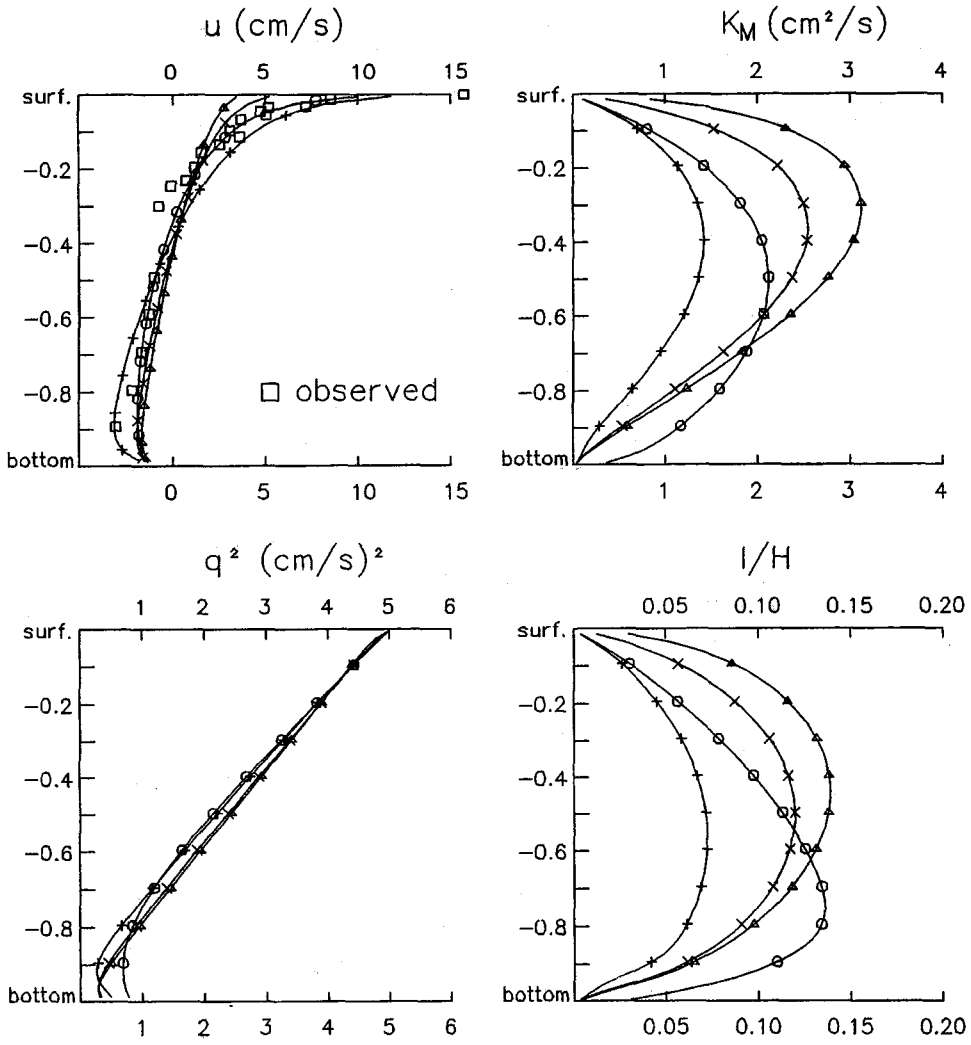

Fig. 3. Profiles of u, K_M, q^2 and l/H for wind-driven currents in wind-driven flow experiment in closed channel. Square symbols are Baines and Knapp (1965)'s experiment data, other symbols are same as Fig. 1.

shear near the surface. The profiles obtained using W3 (RMSE=1.67) are in a fairly good agreement with the observed data. It is noted that a sharp velocity gradient near the surface is satisfactorily reproduced.

Pearce and Cooper (1981) reproduced Baines and Knapp's experimental data using a numerical model. They obtained an excellent current profile with an eddy viscosity profile, which increases linearly from surface and remains constant (2 cm^2/s) below σ=-0.2. It is worth noting that the profile of K_M obtained using W1 is almost similar to those of Pearce and Cooper's. Lee (1996) successfully reproduced the current profile using Prandtl mixing length model with the asymptotic length scale of W 3. It is indicated that the asymptotic profile l=0.31|z| (1+z/h) is an useful alternative to q^2l equation for simple flow conditions.

Flow-controlled channel flow

Tsuruya (1985) has investigated turbulence structure of channel flows without and with wind action through laboratory experiments. In his experiment, the water depth at measuring section was controlled to remain a constant level of 45 cm with mean velocities of 23.8 and 30.3 cm/s. In this study, one case of Tsuruya's experiment (mean current velocity at measuring section A, $\overline{u}|_A$=30.3 cm/s, see Tsuruya (1985) for detailed descriptions of the experiment) was simulated with input parameters: τ_w^x=0, k_f=0.001 (m/s), Δt=0.25 s, Δx=0.25 m and $\Delta\sigma$=0.01. A constant flow-rate is specified at one lateral boundary, and a radiation boundary condition is used at the other lateral boundary. Values of flow-rate and water depth were chosen by trial and error in order to account for

the condition of $\bar{u}|_A$=30.3 cm/s and H=45cm.

Fig. 4 shows profiles of u, K_M, q^2 and l/H obtained using a range of wall proximity functions. The overall variations of u above σ=-0.8 are similar to each other while the velocity gradient near the bottom obtained using W1 are significantly different from others. The best results (RMSE=0.69) were obtained using W3, while relatively poor results (RMSE=1.73) were obtained using W1. The results obtained using W2 and W4 were reasonably good with RMSE=1.29 and RMSE=1.21, respectively.

Unlike the point model experiment for tidal current in an unbounded deep ocean (h=100m), the length scale does not approach to zero near the surface because the vertical diffusion terms in q^2 and q^2l equation are no longer negligible in this shallow channel flow (H=45cm). The length scales obtained using W2 and W4 show profiles similar to Blackadar(1962)'s formula which has a maximum value at the surface.

Once again the wall proximity functions give rise to significant difference in the profiles of l and K_M. However, current profiles are insensitive to the wall proximity functions (and eddy viscosity) except for the case of W1 which reproduces little gradient near the bottom.

Flow-controlled channel flow under adverse wind action

As a final test, the channel flow under adverse wind action has been investigated. The model simulation continued for 200 seconds with same parameters used in c) except for u_{*s}=1.41 cm/s

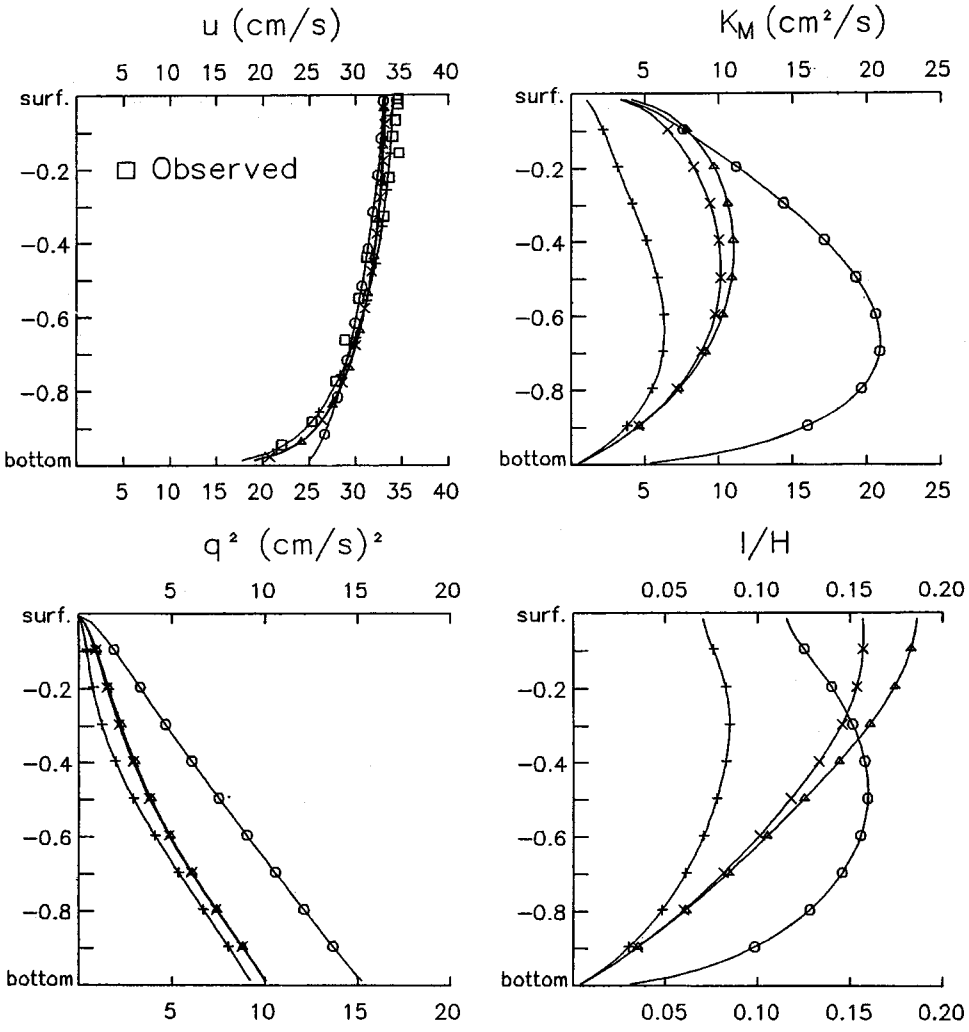

Fig. 4. Profiles of u, K_M, q^2 and l/H for flow-controlled channel flow without wind forcing. Square symbols are Tsuruya (1985)'s experiment data, other symbols are same as Fig. 1.

Table 2. Root mean square errors of velocity (in cm/s) obtained with four wall proximity functions

Wall proximity functions	Wind-driven flow (Baines & Knapp, 1965)	Channel flow without wind (Tsuruya, 1985)	Channel flow with adverse wind (Tsuruya, 1985)
W1	1.41 (0.66)*	1.73	1.80
W2	3.33 (1.97)	1.29	1.86
W3	1.67 (1.47)	0.69	0.72
W4	2.69 (1.38)	1.21	1.70

*Top surface value is excluded (see Fig. 3).

(τ_w^x=-0.2 N/m^2). To determine the linear bottom friction parameter k_f calculation was repeated until u_{*b} reaches 1.35 cm/s which was reported in Tsuruya (1985).

Table 2 summarizes root mean square errors for the laboratory experiments. The best results were obtained in calculation using W3 regardless of wind action, while relatively poor results were obtained using W2 under wind action.

Fig. 5 shows profiles of u, K_M, shear stress and l/H obtained using four wall proximity functions. The overall velocity profiles are similar to each other except for the case of W1 with which vertical shear near the bottom is not well reproduced. The length scale obtained using W3 is similar to its asymptotic length scale, while the length scale profiles with other wall proximity functions show parabolic distribution with respect to water depth.

Without presenting a detailed figure, we briefly describe results of q^2. It is seen that values of q^2 under adverse wind action, as one can deduce from the boundary conditions of q^2, are larger than those without wind action. Surface and bottom values of q^2 with W2, W3 and W4 reach about 11 (cm/s)^2 and 12

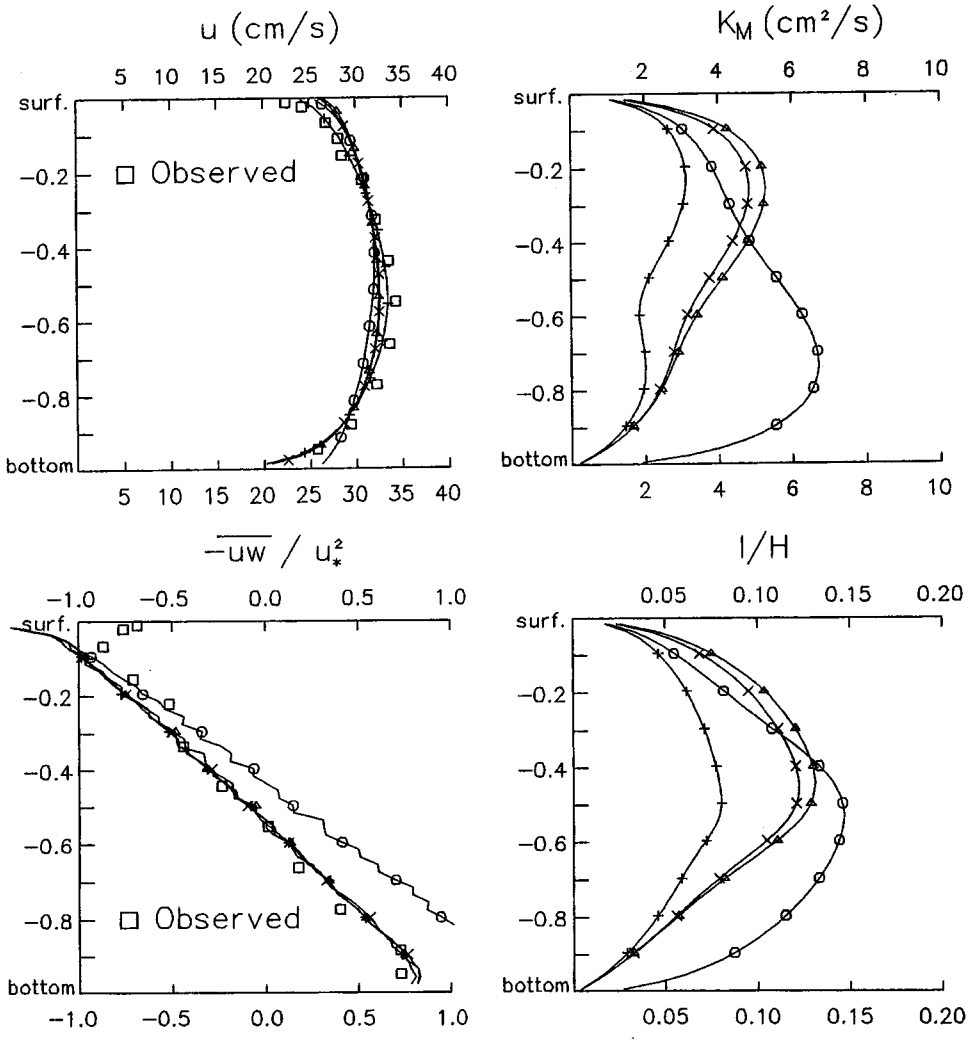

Fig. 5. Profiles of u, K_M, shear stress and l/H for flow-controlled channel flow under adverse wind action. u_* is surface friction velocity. Square symbols are Tsuruya (1985)'s experiment data, other symbols are same as Fig. 1.

$(cm/s)^2$, respectively, while the value of q^2 at mid-depth is about 3 $(cm/s)^2$. On the contrary, in the results with W1 the maximum value of q^2 ($\fallingdotseq$ 22 $(cm/s)^2$) was found at the bottom and u_{*b}=1.35 cm/s was hardly possible with k_f=0.001 (m/s).

The calculated shear stresses (denoted by - $\overline{uw}$ in Fig. 5) below the mid-depth are in a good agreement with Tsuruya's laboratory experiment, however the calculated shear stresses near the surface were significantly different. It is not clear why such discrepancy arises.

CONCLUSION AND DISCUSSION

In homogeneous flows the vertical eddy viscosity K_M is determined by the length scale l and turbulence kinetic energy ($q^2/2$) with a constant deduced from stability function. Calculations show that the wall proximity functions influence by a small amount the turbulence kinetic energy but give considerable difference in the depth-mean values and profiles of l and K_M, affecting significantly the near-surface profiles of wind-driven current, the near-bottom profiles of tidal current and flow-controlled flows and both the near-surface and near-bottom profiles of flow-controlled channel flow under wind action.

The results obtained using W1 (L increasing from the surface) show best performance for wind-driven flow, but relatively poor performance for open-channel flow without wind action. Advantages of using W4 in which asymmetry is enforced are marginal in that vertical shear near the surface is not well reproduced. The length scale obtained using W2 is found to be similar to that obtained using the formula of Blackadar's (1962), and hence its application to pure wind-driven currents is not desirable.

Verification with experimental data shows that the best results can be obtained using a symmetric wall proximity function W3. From practical point of view the length scale calculated with W3 can be approximated by its asymptotic length scale profile l=0.31|z|(1+z/h) without severe sacrifice of accuracy.

Although the MY level 2.5 model with the symmetric wall proximity function shows a fairly good agreement with all experimental data (apparently in cases the boundary layer thickness is equivalent to the water depth), the length scale is physically questionable in that turbulent kinetic energy is not limited by the Ekman layer thickness($\fallingdotseq ku_*/f$). Recall that the ratio of l to H in a shallow wind-driven flow (h=0.328m) is almost identical to that of wind-driven current in an unbounded deep ocean (h=100 m) with turbulence kinetic energies are comparable each other. Investigation on a way of imposing restriction on the length scale is indeed necessary.

ACKNOWLEDGEMENTS

This research was supported by the projects "Development of water quality management for Masan-Chinhae Bay (PE607-1)" sponsored by the Ministry of Science and Technology of Korea and "Development of coastal water quality assessment and prediction technology (PN339)" sponsored by the Ministry of Environments of Korea and by the Ministry of Science and Technology of Korea. The authors appreciate constructive comments from anonymous reviewers.

REFERENCES

Baines, W.D. and D.J., Knapp, 1965. Wind driven water currents. *J. Hydr. Div. ASCE*, **91, HY2**, 205-221.

Blackadar, A.K., 1962. The vertical distribution of wind and turbulent exchange in a neutral atmosphere. *J. Geophys. Res.*, **67**: 3095-3120.

Blumberg, A.F., B. Galperin and D.J., O'Connor, 1992. Modelling vertical structure of open-channel flows. *J. Hydr. Eng., ASCE*, **118(8)**: 1119-1134.

Blumberg, A.F. and G.L., Mellor, 1987. A description of a three-dimensional coastal ocean circulation model. In: Three-dimensional Coastal Ocean Models, edited by N.S. Heaps, Coastal and Estuarine Science 4. American Geophysical Union. Washington, D.C.

Davies, A.M. and J.E., Jones, 1987. Modeling turbulence in shallow regions. In: Small-scale Turbulence and Mixing in the Ocean, edited by J.C.J. Nihoul and B.M., Jamart.

Deleersnijder, E. and P., Luyten, 1994. On the practical advantages of the quasi-equilibrium version of the Mellor and Yamada level 2.5 turbulence closure applied to marine modelling. *Appl. Math. Modelling*, **18**: 281-287.

Galperin, B., L.H., Kantha, S., Hassid and A., Rosati, 1988. A quasi-equilibrium turbulent energy model for geophysical flows. *J. Atmos. Sci.*, **45**: 55-62.

Kantha, L.H. and C.A., Clayson, 1994. An improved mixed layer model for geophysical applications. *J. Geophys. Res.*, **99(C12)**: 25,235-25,266.

Lee, J.C., 1996. Development of a turbulence model for the barotropic shallow seas and its application to the wind-driven circulation of the Yellow Sea and the East China Sea. Ph.D. Thesis, Sung Kyun Kwan University, 241pp (in Korean with English abstract).

Lynch, D.R., T.C., IP Justin, C.E., Naimie and F.E., Werner, 1996. Comprehensive coastal circulation model with application to the Gulf of Maine. *Cont. Shelf Res.*, **16(7)**: 875-906.

Mellor, G.L. and T., Yamada, 1982. Development of a turbulence closure model for geophysical fluid problems. *Rev. Geophys. Space Phys.*, **20(4)**: 851-875.

Mofjeld, H.O. and J.W., Lavelle, 1984. Setting the length scale in a second-order closure model of the unstratified bottom boundary layer. *J. Phys. Oceanogr.*, **14**: 833-839.

Tsuruya, H., 1985. Turbulent structure of currents under the action of wind shear. *J. Hydrosci. and Hydr. Eng.*, **3(1)**: 23-43.

Xing and Davies, 1996. Application of a range of turbulence energy models to the determination M4 tidal current profiles. *Cont. Shelf Res.*, **16**: 517-547.